Journal of Visualized Experiments

Visualizing and Quantifying Endonuclease-Based Site-Specific DNA Damage
--Manuscript Draft--

Article Type:	Methods Article - Author Produced Video
Manuscript Number:	JoVE62175R2
Full Title:	Visualizing and Quantifying Endonuclease-Based Site-Specific DNA Damage
Corresponding Author:	Pankotai Tibor, Habil, Ph.d. University of Szeged, Faculty of Medicine, Institute of Pathology Szeged, HUNGARY
Corresponding Author's Institution:	University of Szeged, Faculty of Medicine, Institute of Pathology
Corresponding Author E-Mail:	pankotai.tibor@szte.hu
Order of Authors:	Vasiliki Pantazi
	Ivett Berzsenyi
	Barbara N Borsos
	Pankotai Tibor, Habil, Ph.d.
Additional Information:	

Question	Response
Please indicate whether this article will be Standard Access or Open Access.	
Please specify the section of the submitted manuscript.	Biology
Please confirm that you have read and agree to the terms and conditions of the author license agreement that applies below:	I agree to the Author License Agreement
Please provide any comments to the journal here.	Nothing
Please indicate whether this article will be Standard Access or Open Access.	Standard Access ($1400)
Please confirm that you have read and agree to the terms and conditions of the video release that applies below:	I agree to the Video Release

1   **TITLE:**
2   Visualizing and Quantifying Endonuclease-Based Site-Specific DNA Damage
3
4   **AUTHORS AND AFFILIATIONS:**
5   Vasiliki Pantazi*, Ivett Berzsenyi*, Barbara N Borsos, Tibor Pankotai
6
7   Institute of Pathology, Faculty of Medicine, University of Szeged, Szeged, Hungary
8
9   * The authors have contributed equally.
10
11   Email Addresses of Co-Authors:
12   Vasiliki Pantazi   (vasiliki.pantazi@med.u-szeged.hu)
13   Ivett Berzsenyi   (berzsenyi.ivett@szte.hu)
14   Barbara N Borsos   (borsos.barbara.nikolett@szte.hu)
15   Tibor Pankotai   (pankotai.tibor@szte.hu)
16
17   Corresponding Author:
18   Tibor Pankotai   (pankotai.tibor@szte.hu)
19

20   **KEYWORDS**
21   DNA repair, chromatin immunoprecipitation, fluorescent microscopy, site-specific DSBs,
22   immunostaining
23

24   **SUMMARY:**
25   This article introduces essential steps of immunostaining and chromatin immunoprecipitation.
26   These protocols are commonly used to study DNA damage-related cellular processes and to
27   visualize and quantify the recruitment of proteins implicated in DNA repair.
28

29   **ABSTRACT:**
30   Cells are continuously exposed to various DNA damaging agents, inducing different cellular
31   responses. Applying biochemical and genetic approaches is essential in revealing cellular events
32   associated with the recruitment and assembly of DNA repair complexes at the site of DNA
33   damage. In the last few years, several powerful tools have been developed to induce site-specific
34   DNA damage. Moreover, novel seminal techniques allow us to study these processes at the
35   single-cell resolution level using both fixed and living cells. Although these techniques have been
36   used to study various biological processes, herein we present the most widely used protocols in
37   the field of DNA repair, Fluorescence Immunostaining (IF) and Chromatin Immunoprecipitation
38   (ChIP), which in combination with endonuclease-based site-specific DNA damage make it
39   possible to visualize and quantify the genomic occupancy of DNA repair factor in a directed and
40   regulated fashion, respectively. These techniques provide powerful tools for the researchers to
41   identify novel proteins bound to the damaged genomic locus as well as their post-translational
42   modifications necessary for their fine-tune regulation during DNA repair.
43

44   **INTRODUCTION**

45   Our genome is constantly being challenged by various DNA damaging agents. These assaults can
46   derive from environmental sources, such as UV light or irradiation, as well as from endogenous
47   sources, such as metabolic by-products caused by oxidative stress or replication errors[1,2]. These
48   lesions can affect the integrity of either one or both DNA strands, and if the generated errors
49   become persistent, it frequently leads to translocations and genome instability, which may result
50   in tumorigenesis[3,4]. To maintain genome integrity, multiple repair systems have been developed
51   during evolution. According to the chemical and physical properties of specific types of DNA
52   damage, multiple repair mechanisms can be activated. Mismatches, abasic sites, single-strand
53   breaks, and 8-oxoguanine (8-oxoG) can be removed either by mismatch repair or base-excision
54   repair pathway[5,6]. Lesions caused by UV-induced photoproducts and bulky adducts can be
55   repaired either by nucleotide-excision repair (NER) or DNA double-strand break repair (DSBR)
56   process[7,8]. NER consists of two main sub-pathways: transcription-coupled NER (TC-NER) and
57   global genomic NER (GG-NER). Regarding the cell cycle phase, following DNA double-strand break
58   induction, two sub-pathways can be activated non-homologous end joining (NHEJ) and
59   homologous recombination (HR)[1,9]. NHEJ, which is the dominant pathway in resting cells, can be
60   activated in all cell cycle phases, representing a faster but error-prone pathway [10]. On the other
61   hand, HR is an error-free pathway, in which the DSBs are repaired based on sequence-homology
62   search of the sister chromatids, therefore it is mainly present in S and G2 cell cycle phases[11].
63   Furthermore, microhomology-mediated end joining (MMEJ) is another DSB repair mechanism,
64   distinct from the aforementioned ones, based on a KU70/80- and RAD51-independent way of re-
65   ligation of previously resected microhomologous sequences flanking the broken DNA ends.
66   Therefore, MMEJ is considered to be error-prone and highly mutagenic[12]. During DNA repair,
67   DSBs can induce the DNA damage response (DDR), which results in the activation of checkpoint
68   kinases that halt the cell cycle during repair[13-15]. The DDR is activated as a response to the
69   recruitment and extensive spreading of initiator key players of the repair process around the
70   lesions, contributing to the formation of a repair focus. In this early signaling cascade, the ATM
71   (Ataxia Telangiectasia Mutated) kinase plays a pivotal role by catalyzing the phosphorylation of
72   the histone variant H2AX at Ser-139 (referred to as γH2AX) around the lesion[16]. This early event
73   is responsible for the recruitment of additional repair factors and the initiation of downstream
74   repair processes. Although the exact function of the recruited proteins at the repair focus has not
75   yet been fully characterized, the formation and the dynamics of repair foci have been
76   investigated by several laboratories. These markers are extensively used to follow the repair
77   kinetics, but their precise role during the repair process remains elusive. Due to the great
78   importance yet poor understanding of DNA repair-related cellular processes, several methods
79   have been developed so far to induce and visualize the DDR.
80

81   Various methods and systems have been established to induce the desired type of DNA damage.
82   For instance, some agents [such as neocarzinostatin (NCS), phleomycin, bleomycin, γ-irradiation,
83   UV] can induce large numbers of random DNA breaks at non-predictive genomic positions, while
84   others (endonucleases, such as AsiSI, I-PpoI or I-SceI, as well as laser striping) can induce DNA
85   breaks at known genomic loci[17-21]. Here, we focus on the endonuclease-based techniques
86   currently used to study the DDR in mammalian and yeast cells. Aside from highlighting the
87   principles of these techniques, we emphasize both their advantages and disadvantages.
88

PROTOCOL

1. Immunodetection of specific proteins

1.1. Preparation of cell culture and experimental setup

1.1.1. Maintain U2OS cells in monolayers in DMEM culture medium supplemented with 10% fetal calf serum, 2 mM glutamine, and 1% antibiotic-antimycotic solution.

NOTE: For endonuclease-based DNA damage induction, use charcoal-treated or steroid-free medium to avoid system leakiness.

1.1.2. Grow cells in a humidified 5% CO_2 environment at 37 °C until 80% confluency, renewing medium every 2–3 days.

1.1.3. Aspirate the medium and wash the cells with 1x PBS. Detach cells with Trypsin-EDTA solution. When the cells detach, stop the trypsin activity by adding culture medium to the cells, yielding a cell suspension.

1.1.4. Count the cells using a cell counting chamber. Plate 2 x 10^4 cells/mL/well on a 24-well plate, with sterile 12 mm round coverslips in each well.

1.1.5. Incubate cells for 24 h at 37 °C in a humidified 5% CO_2 atmosphere to allow attachment onto the coverslips.

1.1.6. Treat the cells with 10 ng/mL of neocarzinostatin (NCS) by directly pipetting the damaging agent to the cultured medium. Incubate the cells with the NCS-containing medium for 15 min, then wash them with 1x PBS and add fresh, supplemented culture medium to the cells. Otherwise, use appropriate agent (i.e., 4-OHT) to induce DSBs via endonuclease-based systems without refreshing the medium[22].

NOTE: Alternatively, use irradiation to induce DNA damage, ranging from 30 min up to 8 h of recovery time by using neutron flux between 2–20 Gy[23].

1.1.7. Incubate cells for 1–8 h at 37 °C in a humidified 5% CO_2 atmosphere to follow the kinetics of DNA repair.

1.2. Fixation of cells

NOTE: 300–500 μL of solutions/well should be used in the following steps (steps 1.1.2-1.1.5) to cover all cells adequately. Each incubation and washing step (except the antibody incubation) should be performed on an orbital shaker with gentle agitation.

1.2.1. Following DSB induction and incubation of cells, remove the medium from the attached

133   cells and wash the cells once with 1x PBS.

134

135   1.2.2. Fix cells with 4% formaldehyde-PBS solution for 20 min at 25 °C.

136

137   **1.3. Permeabilization of cells**

138

139   1.3.1. Remove the fixing solution and wash cells three times with 1x PBS for 5 min each.

140

141   1.3.2. Remove the PBS and add 0.2% Triton X-100 dissolved in PBS. Incubate the samples for 20
142   min.

143

144   **1.4. Blocking of non-specific binding sites**

145

146   1.4.1. Wash the cells three times with 1x PBS.

147

148   1.4.2. Block non-specific binding sites with 5% BSA (Bovine Serum Fraction V albumin) diluted in
149   PBST (1x PBS supplemented with 0.1% Tween-20), and incubate the permeabilized samples for
150   at least 20 min.

151

152   **1.5. Immunofluorescence staining**

153

154   1.5.1. Add the proper amount of primary antibody (i.e., anti-γH2AX, anti-DNA-PKcs) diluted in 1%
155   BSA-PBST solution. Place each coverslip upside down onto a paraffin film over a 10 μL droplet of
156   the diluted anti-γH2AX antibody.

157

158   NOTE: In case of co-immunostaining dilute appropriately both antibodies in the same 1% BSA-
159   PBST solution.

160

161   1.5.2. Incubate the samples in a humidity chamber for 1.5 h at 4 °C.

162

163   NOTE: Incubation can also be performed at 4 °C overnight.

164

165   1.5.3. Place the coverslips back being side up into the 24-well plate and wash three times for 5
166   min with 1x PBS.

167

168   1.5.4. Add the proper amount of secondary antibody diluted in 1% BSA-PBST. Place each coverslip
169   upside down onto a paraffin film over a 10 μL droplet of the diluted antibody.

170

171   1.5.5. Incubate the samples in a humidity chamber at 4 °C for 1 h.

172

173   1.5.6. Place the coverslips back being side up into the 24-well plate and wash three times for 5
174   min with 1x PBS.

175

176   1.5.7. Before removing the last PBS washing solution, gently take out the coverslips using a

177 tweezer and needle and then place them upside down onto glass slides with droplets of mounting
178 medium (supplemented with DAPI).

180 NOTE: Avoid the formation of air bubbles. When the mounting medium dries, it is recommended
181 to seal the edges of the coverslips with nail polish to prevent shriveling of the samples.

183 **2.   Chromatin immunoprecipitation**

185 **2.1. Cell collection, crosslinking, cell and nuclear lysis, and DNA fragmentation**

187 2.1.1. Culture approximately 2×10^7 cells/mL in a 150 mm dish for each sample.

189 2.1.2. Remove the culture medium and wash the cells twice with ice-cold 1x PBS.

191 2.1.3. Fix the cells with 1% formaldehyde-PBS solution, place the plates on an orbital shaker, and
192 agitate gently for 20 min.

194 NOTE: Formaldehyde is volatile; always prepare a fresh working solution. In some cases, the
195 formaldehyde solution contains methanol to stabilize it, but it is better to use a methanol-free
196 solution to avoid interference with downstream reactions.

198 2.1.4. Stop the fixation with 125 mM glycine and incubate on an orbital shaker with gentle
199 agitation for 5 min at 25 °C.

201 2.1.5. Place the plates on ice and wash twice with ice-cold 1x PBS.

203 2.1.6. Scrape the cells in ice-cold 1x PBS and transfer them into 15 mL conical tubes.

205 2.1.7. Centrifuge the cells at 2,500 x g for 5 min at 4 °C.

207 2.1.8. Carefully aspirate the supernatant and resuspend the pellet in 2 mL of cell lysis buffer [5
208 mM PIPES pH 8.0, 85 mM KCl, 0.5% NP-40, 1x PIC (protease inhibitor cocktail)] and incubate on
209 ice for 10 min.

211 2.1.9. Centrifuge the cell suspension at 2,500 x g for 5 min at 4 °C.

213 2.1.10. Carefully discard the supernatant and resuspend the pellet in 500–1,500 µL of nuclear
214 lysis buffer (50 mM Tris-HCl pH 8.0, 10 mM EDTA pH 8.0, 0.8% SDS, 1x PIC) and incubate on ice
215 for 30–60 min. Transfer the lysate into a polystyrene conical tube suitable for sonication.

217 NOTE: Since the nuclear lysis buffer contains SDS, it will precipitate on ice, and the solution will
218 turn white. The solution should turn transparent following sonication.

220 2.1.11. Sonicate the lysate to shear DNA to an average fragment size of 300–1,000 bp.

221

222　NOTE: The appropriate sonication cycles and conditions should be set according to the cell type
223　and the sonication equipment. Fragments smaller than 200 bp are not suitable for ChIP, because
224　the nucleosome-DNA interactions can be disrupted.

225

226　**2.2. Reversal of crosslinking, determination of sonicated fragment sizes**

227

228　2.2.1. Take out 100 µL of the sonicated sample to verify the fragment size of the sonicated
229　chromatin. The remaining chromatin should be stored at −80 °C.

230

231　2.2.2. Add 0.5 mg/mL RNase A to each 100 µL of the sample and incubate them at 37 °C for 20
232　min to activate the RNase.

233

234　2.2.3. Incubate the samples at 65 °C overnight.

235

236　2.2.4. The next day, add 500 µg/mL of Proteinase K and 0.5% SDS, and incubate the samples at
237　50 °C for 3 h.

238

239　2.2.5. Add 0.5 volume of phenol and 0.5 volume chloroform-isoamyl alcohol mix (24:1) to each
240　sample.

241

242　2.2.6. Vortex for 1 min.

243

244　2.2.7. Centrifuge at 13,000 x g for 10 min.

245

246　2.2.8. Transfer the upper aqueous phase to a new microcentrifuge tube.

247

248　2.2.9. Add 1 volume chloroform-isoamyl alcohol mix (24:1) to each sample.

249

250　2.2.10. Vortex for 1 min.

251

252　2.2.11. Centrifuge at 13,000 x g for 10 min.

253

254　2.2.12. Transfer the upper aqueous phase to a new microcentrifuge tube.

255

256　2.2.13. Add 2.5 volumes of 96% ethanol and 0.1 volume of 3 M Na-Acetate pH 5.2.

257

258　2.2.14. Incubate for at least 20 min at −80 °C.

259

260　2.2.15. Centrifuge the samples at 13,000 x g for 10 min at 4 °C.

261

262　2.2.16. Remove the ethanol and wash the pellet with 400 µL of 70% ethanol.

263

264　2.2.17. Centrifuge the samples at 13,000 x g for 10 min at 4 °C.

265

266   2.2.18. Remove the ethanol and air dry the pellet.

267

268   2.2.19. Resuspend the pellet in 10 µL of TE.

269

270   2.2.20. Run the samples on a 0.8% agarose gel. The sonicated chromatin size should be around
271   500 bp.

272

273   NOTE: Use bromophenol blue-free loading buffer because the size of this dye is approximately
274   500 bp, which can disturb the proper detection of chromatin fragments. Instead, it is
275   recommended to use loading buffer complemented with xylene-cyanole, which is approximately
276   3,000 bp.

277

278   2.2.21. If the chromatin size is acceptable, dilute the frozen chromatin samples from step 2.1. in
279   3 volumes of dilution buffer (10 mM Tris-HCl pH 8.0, 0.5 mM EGTA pH 8.0, 1% Triton X-100, 140
280   mM NaCl, 1x PIC) and mix the samples via rotation for 10 min at 4 °C.

281

282   NOTE: This step is necessary to dilute the SDS present in the nuclear lysis buffer to avoid
283   interference with downstream reactions, including the measurement of chromatin
284   concentration.

285

286   2.2.22. Measure the DNA concentration of the chromatin samples at 260/280 nm using a
287   spectrophotometer.

288

289   **2.3. Preparation of beads, pre-clearing, and immunoprecipitation**

290

291   2.3.1. Prepare beads (sheep anti-rabbit or mouse IgG) for the pre-clearing and
292   immunoprecipitation steps. Wash beads twice for 10 min at 4 °C with RIPA buffer (50 mM Tris-
293   HCl pH 8.0, 1 mM EDTA pH 8.0, 1% Triton X-100, 0.1% Na-DOC, 0.1% SDS, 150 mM NaCl and 1X
294   PIC).

295

296   2.3.2. Resuspend the beads in the same volume of RIPA buffer as in step 2.3.1.

297

298   2.3.3. Pre-clear 25–30 µg chromatin of each sample with 4 µL of the beads via rotation for 1–2 h
299   at 4 °C.

300

301   NOTE: Add RIPA buffer to each chromatin sample up to 500 µL of final volume to let the samples
302   mix properly under rotation. Do not forget to take out chromatin for NAC (No Antibody Control)
303   and TIC (Total Input Control) in the case of each sample set. TICs only require a final volume of
304   up to 200 µL.

305

306   2.3.4. Precipitate the beads with a magnet and transfer the supernatant to a new microcentrifuge
307   tube.

308

309   2.3.5. Add the appropriate amount of antibody to each chromatin sample (except NAC and TIC)
310   and rotate overnight at 4 °C.

311

312   2.3.6. Next day, add 40 µL of washed beads to each sample (except TIC) and incubate them
313   overnight, rotating at 4 °C.

314

315   **2.4. Washing**

316

317   2.4.1. Wash once with 300 µL of Low Salt buffer (20 mM Tris-HCl pH 8.0, 150 mM NaCl, 2 mM
318   EDTA pH 8.0, 1% Triton X-100, 0.1% SDS, 1x PIC) for 10 min via rotation at 4 °C.

319

320   2.4.2. Wash once with 300 µL of High Salt buffer (20 mM Tris-HCl pH 8.0, 300 mM NaCl, 2 mM
321   EDTA pH 8.0, 1% Triton X-100, 0.1% SDS, 1x PIC) for 10 min via rotation at 4 °C.

322

323   2.4.3. Wash once with 300 µL of LiCl buffer (250 mM LiCl, 1% NP-40, 1% Na-DOC, 1 mM EDTA pH
324   8.0, 10 mM Tris-HCl pH 8.0, 1x PIC) for 10 min via rotation at 4 °C.

325

326   2.4.4. Wash twice with 300 µL of TE (10 mM Tris-HCl pH 8.0, 1 mM EDTA pH 8.0) for 10 min via
327   rotation, for the first wash at 4 °C, and the second wash at 25 °C.

328

329   **2.5. Elution**

330

331   2.5.1. Add 200 µL of the elution buffer (1% SDS and 100 mM NaHCO$_3$) to the beads and incubate
332   at 65 °C in a thermo-shaker for 15 min with continuous shaking (approx. 400 RPM). Transfer the
333   supernatant to a new tube and elute beads again in 200 µL of Elution buffer. Combine eluates
334   (400 µL final volume).

335

336   2.5.2. Add NaCl to a final concentration of 200 mM in each sample. Supplement the TIC samples
337   with 200 µL of Elution buffer and add NaCl as well.

338

339   NOTE: From this step, TIC should be handled under the same conditions as the other samples.

340

341   2.5.3. Incubate the samples at 65 °C (without shaking) for at least 6 h.

342

343   5.4. Add 1 mL of cold 100% ethanol to each sample, rotate the tubes twice to mix, and precipitate
344   DNA overnight at −80 °C.

345

346   2.5.5. The next day, centrifuge for 30 min at 13,000 x g at 4 °C.

347

348   2.5.6. Discard the supernatant and wash the pellet with 70% EtOH.

349

350   2.5.7. Centrifuge the samples at 13,000 x g for 10 min at 4 °C.

351

352   2.5.8. Discard the supernatant and air dry the pellets.

353

354 2.5.9. Resuspend the pellets in 100 μL of TE and add 0.5 mg/mL of RNase A to each sample.
355 Incubate at 37 °C for 20 min to activate the RNase.

356

357 **2.6. Reversal of crosslinking**

358

359 2.6.1. Add 500 μg/mL of Proteinase K and 0.5% SDS and incubate the samples at 50 °C for 2 h.

360

361 NOTE: If proceeding to ChIP-seq, avoid phenol-chloroform extraction, as it inhibits the
362 downstream NGS process. Instead, it is recommended to use a commercially available kit (see
363 **Table of Materials**).

364

365 2.6.2. Add 0.5 volume of phenol and 0.5 volume of chloroform-isoamyl alcohol mix (24:1) to each
366 sample.

367

368 2.6.3. Vortex for 1 min.

369

370 2.6.4. Centrifuge at 13,000 x g for 10 min.

371

372 2.6.5. Transfer the upper aqueous phase to a new microcentrifuge tube.

373

374 2.6.6. Add 1 volume of chloroform-isoamyl alcohol mix (24:1) to each sample.

375

376 2.6.7. Vortex for 1 min.

377

378 2.6.8. Centrifuge at 13,000 x g for 10 min.

379

380 2.6.9. Transfer the upper aqueous phase to a new microcentrifuge tube.

381

382 **2.7. DNA extraction**

383

384 2.7.1. Add 2.5 volumes of 96% ethanol and 0.1 volume of 3 M Na-Acetate pH 5.2.

385

386 2.7.2. Incubate for at least 20 min at −80 °C.

387

388 2.7.3. Centrifuge the samples at 13,000 x g for 10 min at 4 °C.

389

390 2.7.4. Remove the ethanol and wash the pellet with 400 μL of 70% ethanol.

391

392 2.7.5. Centrifuge the samples at 13,000 x g for 10 min at 4 °C.

393

394 2.7.6. Remove the ethanol and air dry the pellet.

395

396 2.7.7. Resuspend the pellet in 50 μL of TE.

397
REPRESENTATIVE RESULTS
399 Studying site-directed DSB-induced repair processes in cells is performed via either stable or
400 transient transfection. However, it should be noted that stable transfection ensures a
401 homogenous cell population, which gives a unified and thus more reliable cellular response. In
402 the case of transient transfection, only a small proportion of the cell population takes up and
403 maintains the plasmid, which introduces diversity into the experiment. Establishing ER-I-PpoI or
404 ER-AsiSI endonuclease-based cell systems require a 50% confluent cell population, which is more
405 effectively transfected with plasmids encoding the endonuclease. For transfection, commercially
406 available transfection reagents or viral infection-based methods can also be used. If a microscopic
407 visualization technique is to be applied and transient transfection is required, the directed DSBs
408 can be induced by 4-OHT addition 24 h after transfection, which binds to the ER-fused
409 endonucleases and allows the nuclear translocation and DSB induction. To determine the most
410 appropriate time-points, immunofluorescence-based microscopy and western blot detection of
411 γH2AX at different time-points following 4-OHT treatment can be performed. Under physiological
412 conditions, a maximum of 10–15 γH2AX foci per cell can be detected, and the formation of strong
413 repair foci can be triggered by endonucleases (or various other techniques not discussed here
414 e.g., laser microirradiation). A typical I-PpoI endonuclease leads to the formation of elevated
415 γH2AX signals around the nucleolus by inducing DSBs at ribosomal DNA (rDNA). If the breaks are
416 repaired by NHEJ or HR, the number of repair foci decreases over time. For this reason,
417 representative time-points at 0 h, 30 min, 1, 2, 4, and 8 h following 4-OHT treatments are
418 recommended. To track DNA repair processes, the most commonly used cell line is U2OS, as all
419 known repair pathways are fully functional in these cells. When investigating several proteins in
420 the same cells, co-localization can be studied by combining antibodies conjugated with different
421 fluorophores with different emission wavelengths raised in different animal species as shown in
422 **Figure 1**. Therein, the induction of DSBs via an inducible stable cell line is represented which is
423 based on the ER-AsiSI restriction endonuclease fused with hemagglutinin tag (HA). Doxycycline
424 can induce the expression and sequestration of HA-ER-AsiSI in the cytoplasm which can be
425 tracked using an antibody against HA (**Figure 1**. third column, second raw). Incubation for 4 h
426 with 4-OHT, 24 h after doxycycline addition, can induce high number of DSBs since the
427 endonuclease has been translocated to the nucleus (**Figure 1**. third column, third raw and second
428 column, third raw). DSBs can be visualized by using an antibody recognizing γH2AX.
429
430 [Place **Figure 1** here].
431
432 Co-localization of repair proteins at the damage site indicates that they are recruited to the same
433 DNA lesion site, but they do not necessarily interact with each other. The resolution of the
434 confocal microscopy is approximately 300 nm; to determine the binding pattern of specific repair
435 proteins at the break site, super-resolution microscopy (STORM) is instead recommended [24].
436 However, this method requires expensive microscopic equipment and an expert researcher.
437 Alternatively, the binding pattern of the repair proteins can be examined by chromatin
438 immunoprecipitation using DIvA or U2OS-pEP15 stable cell lines, which can express AsiSI and I-
439 PpoI endonucleases in a regulated fashion, respectively[17,21]. Upon 4-OHT addition, both
440 endonucleases can cut the DNA in a sequence specific manner which provides us the opportunity

441 to design locus specific primers to the expected break sites and their surrounding genomic
442 regions. By applying γH2AX antibody in the immunoprecipitation part of the ChIP, we can
443 temporally follow the DNA repair kinetics upon different conditions (such as silencing or
444 inhibition of certain repair factors of interest, i.e., DNA-PKcs). A typical experimental result
445 obtained using ChIP-qPCR is represented in **Figure 2.** Therein, the temporal enrichment of γH2AX
446 is demonstrated as a response to I-PpoI-induced DNA damage. On the left part of the image, the
447 timely detected γH2AX signal is shown at the break site while on the right part, the γH2AX
448 distribution is represented at a control gene region at which DSBs have not been induced.

450 [Place **Figure 2** here]

452 **FIGURE LEGENDS**
453 **Figure 1: Immunofluorescence microscopy is used to detect γH2AX in cultured cells expressing**
454 **HA-ER-AsiSI**. DOX (doxycycline) addition activates the cytoplasmic expression of HA-ER-AsiSI and
455 4-OHT (4-hydroxytamoxifen) (4 h) induces the nuclear translocation of the fusion protein, which
456 leads to the induction of DSBs at known genomic positions. HA (hemagglutinin) staining (anti-HA
457 antibody) represents the HA-ER-AsiSI fusion protein in green, and the induction of breaks is
458 verified by γH2AX staining (anti-γH2AX antibody) in red. Scale bars represent 20 μm.

460 **Figure 2: Temporal enrichment of γH2AX as determined by chromatin immunoprecipitation in**
461 **response to I-PpoI-induced DNA damage**. Left, γH2AX signal at the break site; right, γH2AX
462 distribution at a control region where DSBs were not induced (anti-γH2AX antibody). The
463 represented results are derived from one biological experiment, and error bars indicate the
464 variations of the corresponding sample replicates. N=3.

466 **DISCUSSION**
467 Although DNA repair is a relatively recent research field, our knowledge is rapidly expanding with
468 the help of various biochemical and microscopic methods. Preserving genetic information is
469 crucial for cells since mutations occurring in genes involved in repair processes are among the
470 leading causes of tumorigenesis and therefore elucidating the key steps of DNA repair pathways
471 is essential.

473 Biochemical techniques (i.e., western blot, immunoprecipitation, mass-spectrometry, etc.)
474 require large number of cells and the studied repair processes represent a snapshot of the
475 desired cell population. Performing ChIP experiments is laboring, troublesome and many
476 considerations have to be taken into account when designing specific experiment to study the
477 process of DSB repair. The following steps are some examples: (I) cells should be properly lysed;
478 it is highly recommended to apply a two-step lysation method by using separate cell- and nuclear
479 lysis buffer to ensure higher accessibility to the chromatin fraction (II) chromatin should not be
480 over- or undersonicated; the appropriate conditions of sonication should be optimized to each
481 cell type beforehand (III) the appropriate amount of purified antibody should be determined
482 since antibodies against the same protein from different companies exhibit non-identical
483 characteristics (IV) for the efficient immunoprecipitation, 25-30 ug initial chromatin should be
484 used in each condition (V) the appropriate time of fixation should be optimized, as overfixation

can result in false positive results by cross-linking the distant protein complexes and underfixation can prevent the proper cross-linking between DNA and the desired protein (VI) based on the applied antibody, the type of the beads (protein A or G) should be carefully determined (VII) during washing steps, the order of the washing buffers should be thoroughly kept to avoid the release of the antibody from the beads (VIII) during DNA extraction, phenol traces should be properly eliminated to avoid decreasing the efficiency of the further downstream reactions. Since this method reduces the yield of recovered DNA, our personal advice is to rather use specific DNA-purification kit. When all critical points have been properly addressed, ChIP can provide valuable data for the occupancy of the desired protein at different genomic loci and can unravel critical steps in DNA repair processes.

However, ChIP combined with qPCR is an indirect approach to study the protein distribution at selected genomic regions and does not allow to specifically recognize the DNA binding site nor directly examine the function of the protein. Mono- or polyclonal antibodies used to capture the protein-DNA complexes can also cross-react with other proteins leading to false-positive data and therefore, the antibodies used in this technique should be ChIP-grade and highly specific against the protein of interest. However, ChIP is a widely used technique and further approaches based on this have been developed, such as ChIP-on-chip and ChIP-seq. The former one relies on hybridizing the immunoprecipitated and purified DNA fragments on a microarray with a large variety of small random DNA sequences which further amplifies the annealed sequences providing valuable information about protein binding sites. However, ChIP-seq has emerged as an attractive alternative approach since it provides genome-wide mapping of protein-DNA complexes with higher resolution than ChIP-on-chip and high-throughput genome sequencing. ChIP-seq has revolutionized the field of DNA repair by disclosing DNA binding sites of various transcription factors providing insights into the gene regulation and unravelling chromatin landscapes in a genome-wide scale[25]. According to this, the field of DNA repair has tremendously profited from ChIP-seq since these data play a crucial role in various diseases and biological pathways, such as cancer progression. Nonetheless, various modifications of the ChIP method have been developed such as HaloChIP, which does not require specific antibody against the protein of interest but rather uses sequences encoding DNA-binding proteins fused with HaloTag, which are transfected to cells and subsequently to crosslinking, the desired protein-DNA complexes can be captured by using HaloLink Resin. However, this technique relies on overexpression and not the endogenous level of the desired proteins which can result in misinterpreted data[26].

Furthermore, microscopic techniques provide valuable information about the spatiotemporal tracking of DNA damage repair, even in a single-cell level. The rapid improvement of antibodies raised against specific repair proteins has led to a deeper understanding of the mechanism of NER and DSBR sub-pathways, as well as their post-translational regulation. The microscopic field has been revolutionized by high-resolution techniques, such as super-resolution microscopy, which allows the visualization of DNA damage-induced cellular processes at the nucleosomal level, as well as ensuring the accurate mapping of protein co-localization[24]. However, it should be noted that the variance in cell lineages must be considered during the experiment as the rate of the repair can diverge, which can make the results difficult to interpret. Considering the rapid

529 evolution of fluorescence imaging methodology and the deliberate design of the experimental
530 setup, a precious opportunity to investigate the DNA damage-induced cellular and molecular
531 responses at a single protein resolution in a single-cell level is on its way to perfection.
532
533 In conclusion, the combination of super-resolution microscopy and single-cell sequencing
534 methodology can significantly improve our understanding of the DNA repair field.
535

542

543 **DISCLOSURES:**
544 None
545

546 **REFERENCES**
547 1   Borsos, B. N., Majoros, H. & Pankotai, T. Ubiquitylation-Mediated Fine-Tuning of DNA
548   Double-Strand Break Repair. *Cancers (Basel).* **12** (6), doi:10.3390/cancers12061617
549   (2020).
550 2   Borsos, B. N., Majoros, H. & Pankotai, T. Emerging Roles of Post-Translational
551   Modifications in Nucleotide Excision Repair. *Cells.* **9** (6), doi:10.3390/cells9061466 (2020).
552 3   Stephens, P. J. *et al.* The landscape of cancer genes and mutational processes in breast
553   cancer. *Nature.* **486** (7403), 400-404, doi:10.1038/nature11017 (2012).
554 4   Turnbull, C. *et al.* Gene-gene interactions in breast cancer susceptibility. *Human
555   Molecular Genetics .* **21** (4), 958-962, doi:10.1093/hmg/ddr525 (2012).
556 5   Saxowsky, T. T., Meadows, K. L., Klungland, A. & Doetsch, P. W. 8-Oxoguanine-mediated
557   transcriptional mutagenesis causes Ras activation in mammalian cells. *Proceedings of the
558   National Academy of Sciences of the United States of America.* **105** (48), 18877-18882,
559   doi:10.1073/pnas.0806464105 (2008).
560 6   Jiricny, J. The multifaceted mismatch-repair system. *Nature Reviews Molecular Cell
561   Biology.* **7** (5), 335-346, doi:10.1038/nrm1907 (2006).
562 7   Hanawalt, P. C. & Spivak, G. Transcription-coupled DNA repair: two decades of progress
563   and surprises. *Nature Reviews Molecular Cell Biology.* **9** (12), 958-970,
564   doi:10.1038/nrm2549 (2008).
565 8   Kanaar, R., Wyman, C. & Rothstein, R. Quality control of DNA break metabolism: in the
566   'end', it's a good thing. *EMBO Journal.* **27** (4), 581-588, doi:10.1038/emboj.2008.11
567   (2008).
568 9   Lemaitre, C. *et al.* Nuclear position dictates DNA repair pathway choice. *Genes &
569   Development.* **28** (22), 2450-2463, doi:10.1101/gad.248369.114 (2014).
570 10   Lieber, M. R. The mechanism of double-strand DNA break repair by the nonhomologous
571   DNA end-joining pathway. *Annual Review of Biochemistry.* **79** 181-211,
572   doi:10.1146/annurev.biochem.052308.093131 (2010).

573 11 Lambert, S. & Lopez, B. S. Characterization of mammalian RAD51 double strand break
574 repair using non-lethal dominant-negative forms. *EMBO Journal.* **19** (12), 3090-3099,
575 doi:10.1093/emboj/19.12.3090 (2000).

576 12 Xu, S. *et al.* p300-mediated acetylation of histone demethylase JMJD1A prevents its
577 degradation by ubiquitin ligase STUB1 and enhances its activity in prostate cancer. *Cancer*
578 *Research.* doi:10.1158/0008-5472.CAN-20-0233 (2020).

579 13 Kastan, M. B. & Bartek, J. Cell-cycle checkpoints and cancer. *Nature.* **432** (7015), 316-323,
580 doi:10.1038/nature03097 (2004).

581 14 Roy, R., Chun, J. & Powell, S. N. BRCA1 and BRCA2: different roles in a common pathway
582 of genome protection. *Nature Reviews Cancer.* **12** (1), 68-78, doi:10.1038/nrc3181 (2011).

583 15 Krenning, L., van den Berg, J. & Medema, R. H. Life or Death after a Break: What
584 Determines the Choice? *Molecular Cell.* **76** (2), 346-358,
585 doi:10.1016/j.molcel.2019.08.023 (2019).

586 16 Rogakou, E. P., Pilch, D. R., Orr, A. H., Ivanova, V. S. & Bonner, W. M. DNA double-stranded
587 breaks induce histone H2AX phosphorylation on serine 139. *Journal of Biological*
588 *Chemistry.* **273** (10), 5858-5868, doi:10.1074/jbc.273.10.5858 (1998).

589 17 Caron, P. *et al.* WWP2 ubiquitylates RNA polymerase II for DNA-PK-dependent
590 transcription arrest and repair at DNA breaks. *Genes & Development.* **33** (11-12), 684-704,
591 doi:10.1101/gad.321943.118 (2019).

592 18 Caron, P. *et al.* Cohesin protects genes against gammaH2AX Induced by DNA double-
593 strand breaks. *PLoS Genetics.* **8** (1), e1002460, doi:10.1371/Journal.pgen.1002460 (2012).

594 19 Berkovich, E., Monnat, R. J., Jr. & Kastan, M. B. Assessment of protein dynamics and DNA
595 repair following generation of DNA double-strand breaks at defined genomic sites. *Nature*
596 *Protocols.* **3** (5), 915-922, doi:10.1038/nprot.2008.54 (2008).

597 20 Paques, F. & Duchateau, P. Meganucleases and DNA double-strand break-induced
598 recombination: perspectives for gene therapy. *Current Gene Therapy.* **7** (1), 49-66,
599 doi:10.2174/156652307779940216 (2007).

600 21 Pankotai, T., Bonhomme, C., Chen, D. & Soutoglou, E. DNAPKcs-dependent arrest of RNA
601 polymerase II transcription in the presence of DNA breaks. *Nature Structural & Molecular*
602 *Biology.* **19** (3), 276-282, doi:10.1038/nsmb.2224 (2012).

603 22 Iacovoni, J. S. *et al.* High-resolution profiling of gammaH2AX around DNA double strand
604 breaks in the mammalian genome. *EMBO Journal.* **29** (8), 1446-1457,
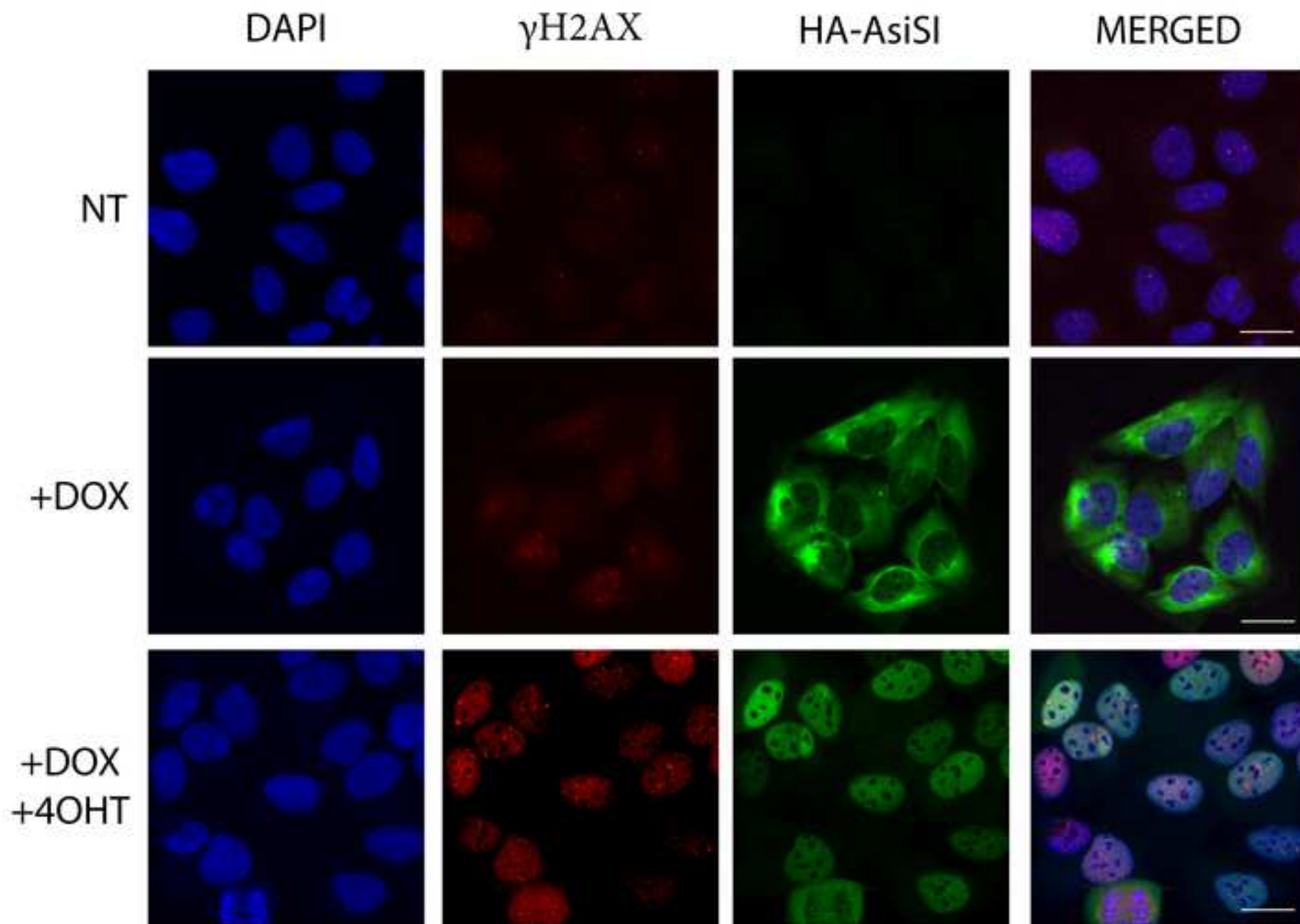605 doi:10.1038/emboj.2010.38 (2010).

606 23 Poinsignon, C. *et al.* Phosphorylation of Artemis following irradiation-induced DNA
607 damage. *European Journal of Immunology.* **34** (11), 3146-3155,
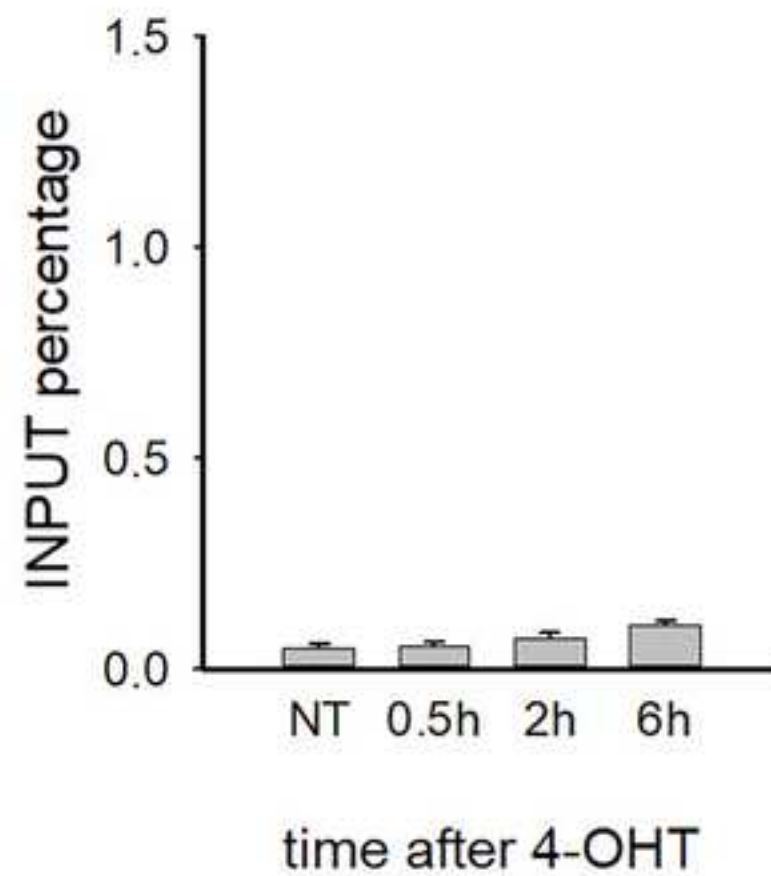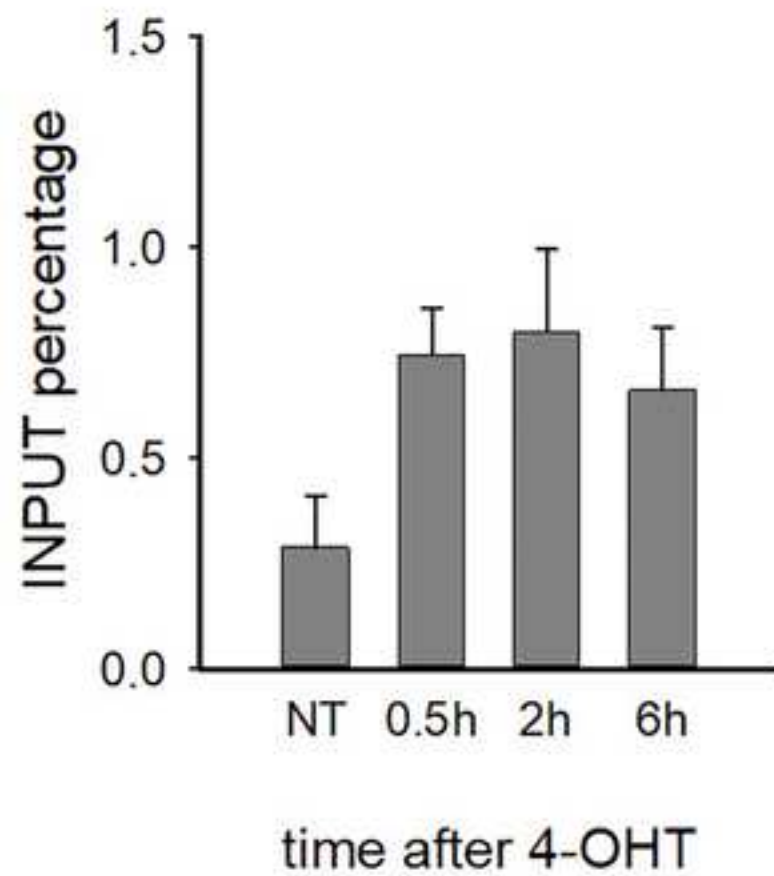608 doi:10.1002/eji.200425455 (2004).

609 24 Varga, D., Majoros, H., Ujfaludi, Z., Erdelyi, M. & Pankotai, T. Quantification of DNA
610 damage induced repair focus formation via super-resolution dSTORM localization
611 microscopy. *Nanoscale.* **11** (30), 14226-14236, doi:10.1039/c9nr03696b (2019).

612 25 Kim, J. A., Kruhlak, M., Dotiwala, F., Nussenzweig, A. & Haber, J. E. Heterochromatin is
613 refractory to gamma-H2AX modification in yeast and mammals. *Journal of Cell Biology.*
614 **178** (2), 209-218, doi:10.1083/jcb.200612031 (2007).

615   26   Daniels, D. L. & Urh, M. Isolation of intracellular protein--DNA complexes using HaloCHIP,
616   an antibody-free alternative to chromatin immunoprecipitation. *Methods in Molecular*
617   *Biology.* **977** 111-124, doi:10.1007/978-1-62703-284-1_9 (2013).

618

Click here to access/download

Table of Materials

JoVE_Materials_Pantazi_Berzsenyi_Final.xlsx

Institute of Pathology
Faculty of Medicine / Clinical Centre, University of Szeged
Director: Prof. Dr. László Tiszlavicz

Állomás utca 1, Szeged, H-6725, Hungary; +36-62-545-148; office.patho@med.u-szeged.hu

Date: 17/05/2021

Dear Dr. Nam Nguyen,

Please find here a revised version of the manuscript entitled '**Visualising and quantifying endonuclease-based site-specific DNA damage**', which was evaluated by three expert reviewers, and based on their opinion, you advised us to revise and resubmit it for publication in *JoVe*.

We thank the critiques and advices that we mostly accepted and modified the interpretation of our data accordingly. We sincerely believe that, as a result of these changes, the quality of our manuscript has been significantly improved, and the present form of the MS will be suitable for publication in *JoVe*. Our responses to the Editorial comments are provided here.

In short, the changes we introduced into the new version of the manuscript are as follows:
- We have made modifications in the text based on the recommendations of the Editor.
- We have modified the video and the narration accordingly to increase the homogeneity between the video file and the written manuscript. In the current form of the video and the written manuscript reflecting of each other.
- We have inserted chapter title cards and we applied American English spelling.
- We have removed commercials from the text and from the narration.
- We have added the requested chapters to the video file (result and conclusion. We also re-organized the chapter according to the request of the Editor.
- We have changed the narration accordingly.

We declare that our manuscript has not been submitted for publication elsewhere.
We thank all the Reviewer's comments and your editorial contribution to the publication of this work.

We are looking forward to hearing your positive response.

Sincerely,

Tibor Pankotai

Tibor Pankotai, Ph.D.
Research fellow and Principal Investigator
Institute of Pathology, University of Szeged
1, Allomas street Szeged H6725, HUNGARY
e-mail: pankotai.tibor@szte.hu